Comparación de Modelos de Electrones Libres

Aarnav Panda, Max Behrens, Grupo 13

Facultad de Ciencias

Universidad Autónoma de Madrid

Informe del Cuarto Curso

Diciembre 2024

Abstract

This report uses simulations to investigate via the variation of experimental parameters what differences lie between the Drude and Sommerfeld models for the behaviour of electrons in metals. The Hall effect, drift velocity and noise of the systems are evaluated and compared to theoretical predictions under various temperatures and scattering rates.

1 Introduction

1.1 Development of Free Electron Models

At the turn of the 19th century, the Drude and Sommerfeld models were early attempts of predicting the prominent characteristics of metals. Paul Drude developed his model prior to even the confirmation of the existence of atoms, supposing only that electrons scattered off of positive regions. [1] He succeeded, partly through luck, in providing a theoretical explanation for the Wiedemann-Franz law and partially for other quantities such as the Hall coefficient. [2]

The Drude model assumes a classical gas of electrons, so the natural continuation with the arrival of quantum physics was to account for the fermionic nature of electrons. Arthur Sommerfeld, leaving the other assumptions of the Drude model intact, replaced the classical Maxwell-Boltzmann statistics with Fermi-Dirac statistics and was able to accurately explain the electronic heat capacity of the methods [3]. However, limited by the non-inclusion of phonons and the neglecting of lattice potentials, the two models were ultimately unable to fully explain properties such as the full heat capacity in the low temperature limit, which was refined to a much greater extent in the Debye model.

By varying parameters concerning temperature, collisions and applied fields, the significance of this difference in the classical and quantum models is observed as variation in the drift velocity and noise, and compared to the theoretical predictions for behaviour.

1.2 The Solid State Simulation (SSS) Project

The SSS project, developed by Cornell, is employed for the modelling of the Drude and Sommerfeld models.[4] Use is made of the accompanying information and presets to identify relevant quantities [5]. The program covers a very large parameter space, and as such only small, selective ranges have been tested for efficacy.

From the Drude model, the parameters of mean square deviation and mean value are logged for both position and velocity in 2D. E and B fields are applicable, and the scattering time τ is a controllable parameter. A critical parameter is the temperature T_D, which sets the characteristic temperature of the Maxwell-Boltzmann distribution from which the electrons velocities are simulated.

From the Sommerfeld model, the x and y components of the average wave vector $\langle \mathbf{k} \rangle$, are logged together with the excess energy of the electrons. E and B fields are applicable, and the inelastic and elastic scattering times τ_i and τ_e are tunable.

With respective to the quantum nature of the model, the density of k-space - and thereby the number density - is adjustable through the "box size" in Angstroms. Finally, the Fermi energy E_F is given for a small range of eV. The average energy lost per inelastic collision, ΔE, is also a tuneable parameter in units of eV.

2 Theory of free electron models

2.1 Drude

The key assumptions of the Drude model are vastly simplifying[2]:

- **Independent electrons:** Electrons are non-interacting with each other.
- **Free electrons:** Electrons are not subject to a potential, neither between each other nor with the lattice.
- **Collisions:** Electrons only collide instantaneously with the ionic cores, and only reach thermal equilibrium through collisions.
- **Relaxation Time:** Collisions may be modelled with a Poisson distribution with expectation value τ^{-1} (i.e. the scattering rate).

- **Classical Gas:** Electrons are modelled classically with Maxwell-Boltzmann statistics.

Using the Drude model, a successful rudimentary explanation of electron conductivity can be made, however, the equipartition theorem tells us that we ought predict that the electronic heat capacity to be

$$C_e = \frac{3}{2} n k_B \tag{1}$$

where n is the electron number density. This prediction deviates significantly from experimental data, particularly at low temperatures. It is in this area that the Sommerfeld model offers a drastic improvement.

2.2 Sommerfeld

The shortcomings of the Drude model stem partly from its reliance on classical kinetic theory, which fails to consider the quantum mechanical nature of electrons. In the Drude model, all electrons - as classical particles - are able to increase in energy. In reality, this is only true of electrons near the Fermi surface, which are capable of being excited into vacant energy states. The opposite is true: they are also incapable of relaxing into occupied energy levels of lower momenta, which has implications for inelastic scattering events.

By incorporating the Fermi-Dirac distribution, the Sommerfeld expansion offers a more accurate approximation of the temperature dependence, T, of the electron energy, U. At low temperatures, the series converges rapidly, allowing higher-order terms to be neglected. For a 2D Fermi gas, this leads to:

$$U(T) = \frac{nE_F}{2} + \frac{n\pi^2}{6E_F}(k_b T)^2 \tag{2}$$

where n is the electron number density, k_b is the Boltzmann constant and E_F is the Fermi energy [6]. It is evident that the specific heat now exhibits a temperature dependence, proportional to T, a feature absent in the Drude model, equation 3:

$$C_e = \frac{n\pi^2 k_b^2}{3E_F} T \tag{3}$$

This expression provides a significant improvement over the Drude model and aligns much better with experimental observations. It represents a key step toward the modern, widely accepted heat capacity model derived from the Debye theory:

$$C_e = \gamma T + AT^3 \tag{4}$$

where γ and A are empirical constants specific to the material, with γT accounting for the electronic contribution and AT^3 capturing the lattice vibrations [6].

2.3 Comparison of velocity distributions

The key difference in the two models, aside from the discretisation of energy levels and Pauli exclusion principle, is primarily expressed in the different velocity distribution. In this subsection the differing behaviours across a range of temperatures is qualitatively analysed.

The Drude model operates under a Maxwell-Boltzmann distribution, with a memoryless property for electrons that chooses a new velocity from the distribution for the electron post-collision. The occupancy in a classical gas is given by

$$\bar{n}_{MB}(\varepsilon_i) = \frac{1}{e^{(\varepsilon_i - \mu)/k_B T_D}}, \tag{5}$$

where ε_i denotes the energy of a given state, and μ the chemical potential. By comparison, a Fermi-Dirac occupancy function is given as [7]

$$\bar{n}_{FD}(\varepsilon_i) = \frac{1}{e^{(\varepsilon_i - \mu)/k_B T} + 1}. \tag{6}$$

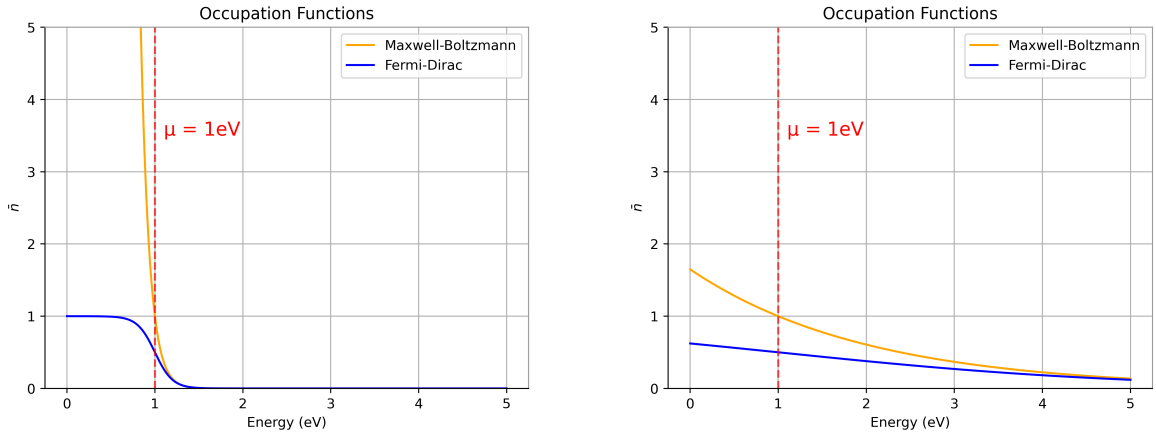

(a) Low temperature regime

(b) High temperature regime

Figure 1: Plot of the occupancy function in the different limits for temperature for Maxwell-Boltzmann and Fermi-Dirac distributions.

In the low temperature regime the most significant deviation is observed; the classical predictions of the Drude model are hindered by the inaccurate prediction of the occupancy of very low energy states. The Maxwell-Boltzmann distribution here is overly likely to predict the energy, and hence the velocity, of an electron to be too low, which will also influence the predictions of electronic conductivity.

Within the SSS project 'drude' model simulation, electron collisions are governed according to the scattering rate τ^{-1}, where τ is the scattering time. After a collision, the program chooses a velocity from the Maxwell-Boltzmann distribution, using the parameter T, and a random orientation for the electron.

As discussed in Section 2.2, only the electrons near the Fermi surface are capable of being excited, and the energy available for such excitations is on the order of $k_B T$. At higher temperatures, the classical prediction becomes less inaccurate, as $k_B T$ grows much larger than the energy gaps between levels, causing the velocity space to appear more continuous. In this regime, the effects of quantization and the Pauli exclusion principle become less significant. Consequently, the results from both the classical and quantum models should converge at higher temperatures, producing similar outcomes.

3 Sommerfeld Temperature

While the Drude model includes a direct temperature parameter, the Sommerfeld model does not. Temperature is instead indirectly controlled by adjusting the ΔE and collision parameters. Fixed simulation parameters are chosen, with the Fermi energy set to 10 eV and the lattice constant to 50 Å for all simulation runs in this report.

The Sommerfeld simulation program calculates the excess energy, E_{excess}, as a function of time, defined as the difference between the average energy at time t and the initial average energy. At the start of the simulation, all electrons are within the Fermi sphere (k_F), and the initial average energy corresponds to the absolute zero value, calculated for a 2D Fermi gas as

$$\langle E(0)\rangle = \frac{E_F}{2}. \tag{7}$$

At equilibrium, the internal energy of the electron gas is given by

$$U(T) = N(\langle E(0)\rangle + \langle E_{excess}(T)\rangle), \tag{8}$$

where $\langle E_{excess}(T)\rangle$ represents the average excess energy at equilibrium for temperature T. Comparing Equation 8 with Equation 2, we identify the excess energy at low temperatures to be

$$\langle E_{excess}(T)\rangle = \frac{\pi^2 k_b^2}{6E_F}T^2. \tag{9}$$

Via substitution into Equation 9, it is seen that to model metals at low temperatures (e.g., 20 K), a value of $\langle E_{excess}(T)\rangle \sim 10^{-7}$ eV is required. A relation between simulation parameters and excess energy is necessary in order to control the temperature of the simulation.

The Sommerfeld model allows control of both elastic and inelastic collisions. Elastic collisions conserve the total energy of the system, butthe behaviour of inelastic collisions is governed by the simulation parameter ΔE - the average energy loss during such a collision. During an inelastic collision, an electron will either lose energy on the scale of ΔE - provided there is an available energy level for the transition - or gain energy on an independent scale, denoted as $\Delta E'$. This energy scale is an inherent aspect of the system and related to the density of states. An electron will preferentially lose energy in an inelastic collision, and will only gain energy if it is unable to drop to a vacant state. This relation is explored briefly in more detail in Appendix A, where it presents an interesting nuance.

Consequently, elastic collisions enable the electrons to gain energy until equilibrium is established between ΔE and $\Delta E'$. It can also be inferred that the system's energy gain rate will be dependent on the ratio of the frequency of elastic and inelastic collision times, $R_\tau = \tau_e/\tau_i$.

The minimum excess energy ($\sim 10^{-2}$ eV), found in Figure 5, Appendix A is insufficient for low-temperature modelling, as it remains several orders of magnitude too large. In theory, R_τ could be set to a very low value, allowing excess energy to increase gradually until it reaches the desired level, after which it could be maintained. However, the simulation software does not permit the precision required to resolve $\langle E_{excess}(T)\rangle \sim 10^{-7}$ eV, as only graphical data is readily available. Therefore, the temperature of the Sommerfeld simulation program cannot be controlled at low enough excess energies to accurately use equation 9 [5].

Using the available software, an approximate low temperature regime can be established by setting $\tau_e >> \tau_i$ and prohibiting energy gain through inelastic interactions. In contrast a high temperature can be achieved by introducing a non-negligible τ_i. No precise value of temperature can be determined in these regimes, which impacts the ability to compare the noise values discussed in Section 4.

4 Static Noise Comparison

The noise of the simulation is defined as the variation of $\langle \mathbf{v} \rangle$ over the course of its runtime. The noise originates from the probabilistic nature of the distribution discussed in Section 2.3, and is expected to exhibit the largest difference at low temperatures. To investigate this, the noise of the two simulations were compared in the absence of electromagnetic fields, across both high and low temperature regimes.

4.1 Low Temperature

The Drude model temperature can be controlled directly, and was set to 1 K. As discussed in section 3, the Sommerfeld simulation does not have this freedom, but a low temperature model can be approximated by setting $\tau_i >> \tau_e$. For this investigation both τ_e and τ were set to 1 ps for the Sommerfeld and Drude model, respectively. Both simulations were run 5 times for 100 ps, and the standard deviation of $\langle \mathbf{v} \rangle$ calculated for each run. The averages and the standard error on the noise are presented in Table 1:

Model	**Noise ($\mathbf{ms^{-1}}$)**
Drude	506.3 ± 126.6
Sommerfeld	1497 ± 922.4

Table 1: Low temperature data. Noise($\sigma_{\langle v \rangle}$) is 196% greater in the Sommerfeld model, with significantly more uncertainty.

The increased noise observed in the Sommerfeld model, compared to the Drude model, can be attributed to the differing collision dynamics inherent in each simulation. At low temperatures, the Maxwell-Boltzmann distribution is very narrow, meaning that upon collision, the resulting velocity of the electron lies within a tight range, thereby producing minimal noise in the Drude model. In contrast, the Sommerfeld model considers elastic collisions where the electron is assigned a new **k**-vector with the same magnitude but a random direction[5]. Due to the discrete nature of allowed states, which form a grid-like structure, it is highly unlikely that the new **k**-vector will exactly match one of these allowed states. As a result, the simulation assigns the nearest available state, which in turn can cause a small but systematic energy shift, contributing to the overall heating of the system. To mitigate this, the simulation tracks the discrepancy between the actual **k**-vector and the assigned one, attempting to minimize the difference over multiple collisions. However, under the simulation conditions employed, achieving this balance proves to be challenging, ultimately leading to a higher amount of noise as a result.

4.2 High Temperature

To investigate the high-temperature regime, the Drude model was simulated with a temperature parameter set to 100 K and a collision time of 1 ps. For the Sommerfeld model, both τ_i and τ_e were set to 2 ps to ensure an effective total collision time of 1 ps. The same measurements performed in the low-temperature regime were repeated under these conditions, and the results are summarized in Table 2.

Model	**Noise ($\mathbf{ms^{-1}}$)**
Drude	14210 ± 663.2
Sommerfeld	7553 ± 412.0

Table 2: High temperature data. T is not constant between measurements of $\sigma_{\langle v \rangle}$ and cannot be compared other than holistically.

At higher temperatures, the Maxwell-Boltzmann distribution becomes broader, leading to a corresponding increase in noise within the Drude model. The Sommerfeld model also exhibits a rise in noise, as anticipated, due to the introduction of inelastic collisions. However, it is important to note that a direct comparison of the values between the two models is not feasible, as the temperature in the Sommerfeld model remains unspecified.

5 Comparison of Drift velocity

In this section a comparison of drift velocities of the Drude and Sommerfeld models will highlight the key differences in their treatment of temperature-dependent mechanics. The equations of motion for a free electron gas subjected to an electric field, $\mathbf{E}$, with a collision rate of $1/\tau$, yield the following relation between the steady-state drift velocity, $\mathbf{v}$, and $\mathbf{E}$:

$$\mathbf{v} = -\frac{e\tau}{m_e}\mathbf{E} \tag{10}$$

where e is the electric charge of an electron, and m_e is the mass of an electron[7]. Equation 10 implies a constant relation for all $\mathbf{v}$ and $\mathbf{E}$ at a given τ. This holds true in the Drude model, where τ represents a single inelastic collision parameter. However, in the Sommerfeld model, τ depends on both elastic and inelastic collisions, with the total relaxation time determined by the harmonic sum of the two contributions[4]. This introduces a temperature-dependent modification to the drift velocity.

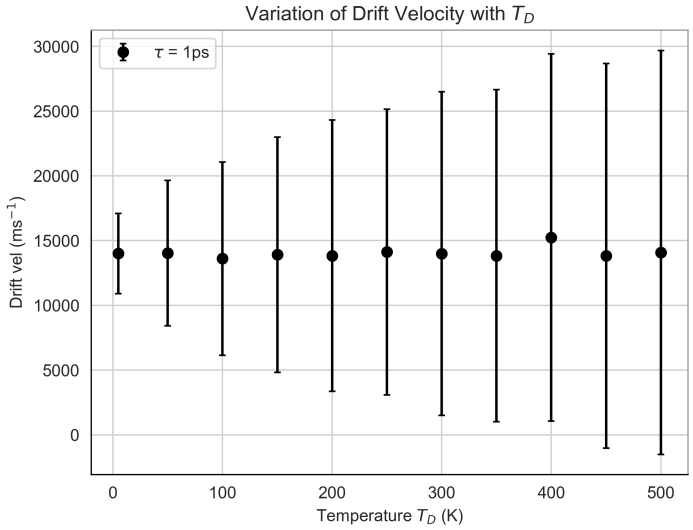

Figure 2: A plot of electron drift velocity in the Drude sim for various values of T_D. The weighted average is $v = 13998 \pm 2185$ ms^{-1}, which has an error of 15.6%.

To verify that temperature does not influence drift velocity in the Drude model, simulations were conducted over a temperature range of 5 K $< T <$ 500 K, with a fixed electric field of 10^4 Vm^{-1}. As can be seen in Figure 2, the increased temperature increases the deviations between collisions, as the electrons are able to move faster in the interval. However, whilst the uncertainty increases, the low percentage uncertainty in the weighted average value for v indicates an overall independence of drift velocity with respect to temperature. The increase in velocity fluctuations is observed at higher temperatures, which can be attributed to the broadening of the Maxwell-Boltzmann distribution $P(x, y; t) = \frac{1}{2\pi\sigma} \exp\left(\frac{x^2+y^2}{2\sigma^2}\right)$, whose spread is given by

$$\sigma^2 = \sigma_0^2 + 2k_B T_D \tau \cdot t, \tag{11}$$

where σ_0, the RMS width is chosen arbitrarily by SSS to be 0.17×10^{-12} m^{-1}. For subsequent analyses, T_D was set to 1 K to minimize thermal fluctuations.

The dependence of $\mathbf{v}$ on $\mathbf{E}$ was further investigated for a fixed τ of 1 ps and electric field strengths ranging from 10^6 Vm^{-1} to 10^7 Vm^{-1}. Drude model simulations were performed using 32 particles,

with the drift velocity averaged over a 1000 ps interval. The total runtime was divided into five equal segments, and the mean drift velocity for each segment was computed. The final value of $\langle \mathbf{v} \rangle$ was obtained by averaging across these segments, with the standard deviation taken as the error. For the Sommerfeld model, simulations were run for various values of R_τ, ensuring that the harmonic sum of the elastic and inelastic collision times remained fixed at 1 ps. Figure 3 presents the results, where the dashed orange line corresponds to the theoretical gradient derived from equation 10, -0.176 $\mathrm{m^2V^{-1}s^{-1}}$.

The Sommerfeld model can be seen to approach the Drude model as R_τ decreases. This is consistent with the discussion in Section 2.3, where it was noted that the velocity distributions differ less as the temperature increases. When only elastic collisions are present, the electric field continuously imparts energy to the electrons, but since the electrons cannot lose energy through collisions, the electron gas keeps heating up. As the electron gas becomes hotter, its velocity distribution increasingly resembles that of the Drude model.

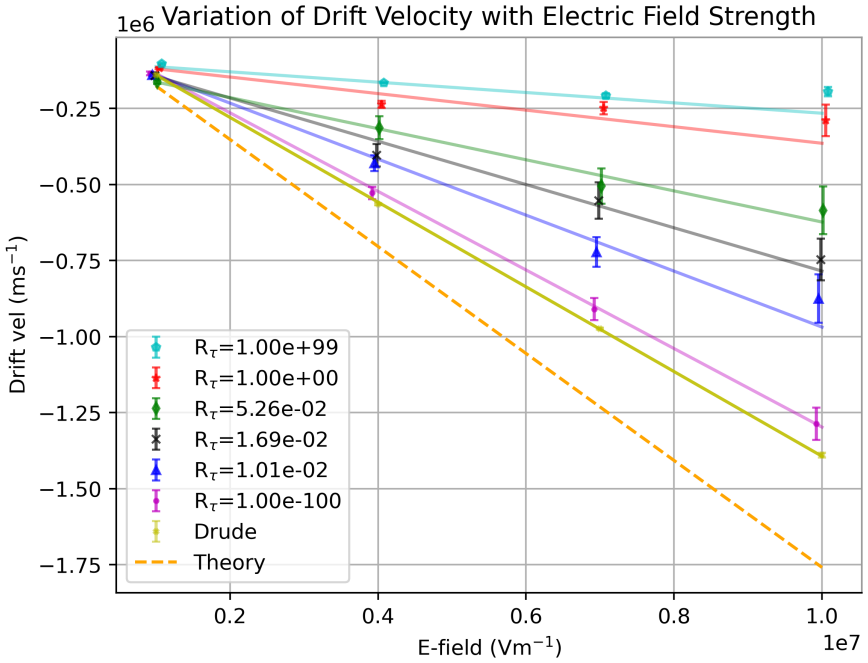

Figure 3: A plot of electron drift velocity against the strength of the applied E field. Points are linearly fit for each data set. For visibility, points are slightly offset, but are taken at values of E = 0.4, 0.7, 1.0 x10^7 Vm^{-1}. The percentage deviation of the closest fit (from the Drude model) from the theoretical prediction was 26.3%. Gradients for R_τ and Drude are found from fitting as $m_D = -0.1292 \pm 0.0009$ and $m_D = -0.1393 \pm 0.0007$ respectively, theory $= 0.175$

Both simulations deviate from the theoretically expected value in their most extreme cases. After extensive investigation into the mechanisms of the modelling, it is unclear where exactly this error arises from. As previously mentioned, the modelling of collisions is largely an open choice for the Drude and Sommerfeld models, and it is possible that the unclear temperature dependence of the inelastic scattering parameter is the problem; in the most extreme cases R_τ is almost zero, implying that there is an additional factor missing in the case of pure inelastic scattering. This is yet to be determined.

6 Hall Angle

The Hall effect describes the generation of a transverse voltage across a conductor when it is placed in a magnetic field perpendicular to the current. This effect is characterized by the Hall angle, ϕ, which represents the angle between the electron velocity components, and is given by the equation [7]:

$$\phi = \tan^{-1}\left(\frac{v_y}{v_x}\right) = \tan^{-1}\left(\frac{B\tau e}{m_e}\right), \tag{12}$$

where v_x and v_y are the x and y velocity components. To investigate this effect, simulations were performed for various values of $B\tau$ ranging from 0.1 Tps to 20 Tps, with the x and y velocity components averaged over time.

The Drude model simulations were carried out with T_D fixed at 30 K, an electric field strength of 10^6 Vm^{-1}, and 32 particles. For the Sommerfeld model, three distinct R_τ values were used to achieve the required collision times for each data point, ensuring consistency across measurements. The results, presented in Figure 4, closely align with the theoretical prediction of equation 12.

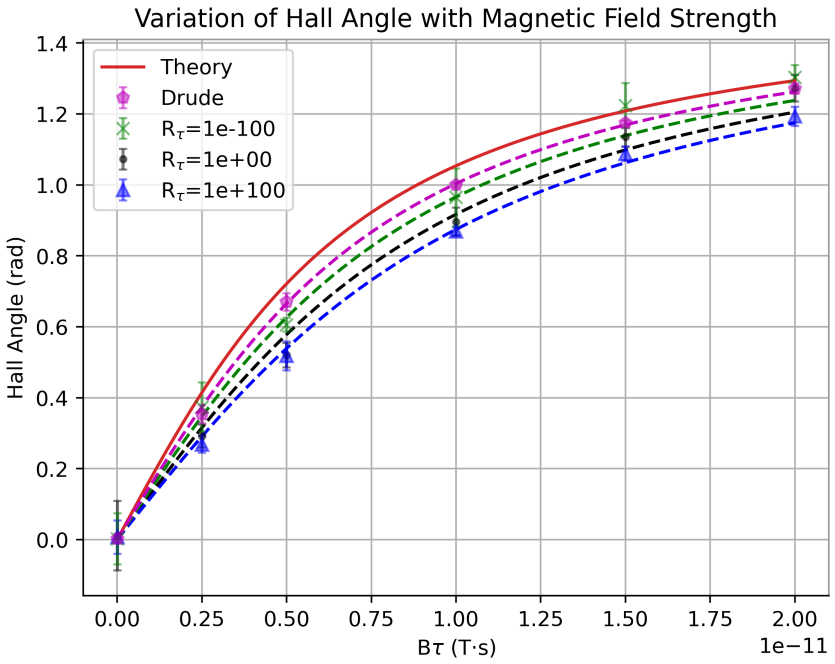

Figure 4: The plot shows the stated relation in Equation 12 for various values of R_T.

R_τ	$\alpha \pm \sigma_\alpha$ (%)
1.00×10^{100}	68.012 ± 1.3441
1.00×10^{0}	74.195 ± 2.8027
1.00×10^{-100}	82.244 ± 2.9688
0^*	89.229 ± 0.84407

Table 3: Fitted values of (α) with uncertainties for various values of (R_τ). *This data point is from the Drude model, which has no elastic collisions and therefore a value $R_\tau = 0$. α is a dimensionless scaling parameter for e/m_e and is expressed as a percentage to indicate the effective value of e/m_e. For the theoretical prediction, $\alpha = 100\%$

As R_τ decreases, the agreement between the theoretical predictions in Figure 4 and Table 3 diminishes. This behaviour can be understood by examining how the collision parameters determine the probabilities of elastic and inelastic collisions.

The probability of an elastic collision is always given by the ratio of the time step to τ_e. For inelastic collisions, this probability is similarly given by the time step divided by τ_i for electrons inside the Fermi sphere. However, for electrons outside the Fermi sphere, the probability of inelastic collision is increased by a factor of E/E_F. This amplification in the collision probability reduces the overall collision time of the simulation.

Therefore, when R_τ is large, inelastic collisions dominate, leading to a reduction in the effective collision time and hall angle. On the other hand, for small values of R_τ, elastic collisions dominate, leading to a closer agreement with theoretical expectations.

7 Conclusions

The deviations between the Drude and Sommerfeld models owing to the differences in velocity distributions and scattering parameters were found in various areas. The noise of the models differed by a factor of nearly 200% in the low temperature limit, and grew significantly as expected in the high temperature limit. Direct comparisons could not be made accurately, due to the lack of precise temperature control in the Sommerfeld simulation. The drift velocity was found to vary as a function of R_τ, the scattering rate ratio, where a dominant rate of elastic scattering under the electric field in the Sommerfeld simulation allowed it to approach the higher temperature limit, where as shown in Section 3, the distributions were similar at high energy. Both the Drude and Sommerfeld model at $R_\tau \sim 0$ had a discrepancy of 26.3%, very significantly greater than 3σ, where σ is the uncertainty on the fit parameter for the gradient of the fitted linear plots. The Hall angle was measured and found to depend loosely on R_τ. The uncertainty from the fit parameter α was used to estimate that the fits were 5.98σ and 12.8σ away from the theoretical predictions, which is a significant difference, similar to for the drift velocity. To improve the accuracy of the simulations, the mechanisms of the scattering rate could be more accurately modelled to explicitly depend on temperature and a greater number of particles could be modelled (noting that this would require greater computational power and more time).

References

[1] P. Drude, "Zur elektronentheorie der metalle," *Annalen der physik*, vol. 306, no. 3, pp. 566–613, 1900.

[2] N. W. Ashcroft and N. D. Mermin, *Solid State Physics*. New York: Holt, Rinehart, and Winston, 1976, ch. 1.

[3] A. Sommerfeld, "Zur elektronentheorie der metalle auf grund der fermischen statistik: I. teil: Allgemeines, strömungs-und austrittsvorgänge," *Zeitschrift für Physik*, vol. 47, pp. 1–32, 1928.

[4] C. University, *Simulations for solid state physics: An interactive resource for students and teachers*, CD-ROM included with the book, published by Cambridge University Press, 1995.

[5] R. H. Silsbee and J. Dräger, *Simulations for Solid State Physics: An Interactive Resource for Students and Teachers*. Cambridge, UK: Cambridge University Press, 1997, Includes CD-ROM, ISBN: 0521590949.

[6] N. W. Ashcroft and N. D. Mermin, *Solid State Physics*. New York: Holt, Rinehart, and Winston, 1976, ch. 2, pp. 44–49.

[7] C. Kittel and P. McEuen, *Introduction to Solid State Physics*, 8th. John Wiley & Sons, 2005, pp. 135–167.

8 Appendix A: Temperature in the Sommerfeld Simulation

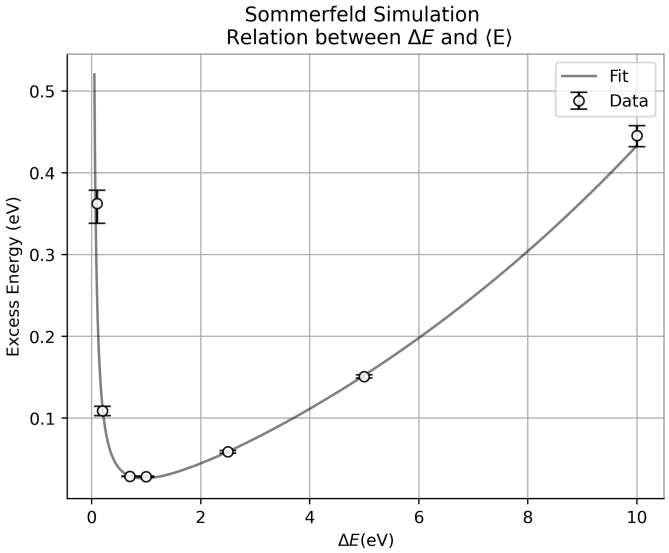

Figure 5: The plot shows the average excess energy of a simulation run for 7 different values of ΔE. The fit is for clarity only.

The relationship between excess energy, hence temperature, and ΔE, was explored by measuring $\langle E_{excess}(T)\rangle$ for 0.1 eV $< \Delta E <$ 10 eV, as shown in Figure 5. Elastic collisions do not contribute to the heating of the gas, therefore, simulations were run until equilibrium was reached for $\tau_i = 10^{-2}\ s, 10^{-1}$ s, 10^0 s, and 10^1 s, and a negligible τ_e. Error bars represent the range of measured values, and confirm that $\langle E_{excess}(T)\rangle$ is independent of τ_i. The data was fitted with a combination of exponential and inverse functions for clarity.

The shape of the graph can be understood by considering the two extreme cases. For $\Delta E << \Delta E'$, particles on average gain more energy than they lose, resulting in higher overall excess energy. For large ΔE, fermion statistics limits energy loss, again leading to a net energy gain. The data exhibits a minimum around $\Delta E \sim 1$ eV. For all measurements, ΔE was fixed at 1 eV to minimize $\langle E_{excess}(T)\rangle$.

9 Appendix B: Data

Data was recorded and organised in a publically accesible github repository, located at:
https://github.com/MaxBehrens1/Solid-State-Project.